Immunoelectron microscopy of low density lipoproteins yields a ribbon and bow model for the conformation of apolipoprotein B on the lipoprotein surface

Jon E. Chatterton,[1],* Martin L. Phillips,* Linda K. Curtiss,† Ross Milne,§ J-C. Fruchart, and Verne N. Schumaker[2],***

Department of Chemistry and Biochemistry and the Molecular Biology Institute,* University of California, Los Angeles, CA 90095; Research Institute of Scripps Clinic,† La Jolla, CA 92037; Lipoprotein and Atherosclerosis Group,§ Room H460, University of Ottawa Heart Institute, Ottawa Civic Hospital, 1053 Carling Avenue, Ottawa, Ontario, Canada K1Y 4E9; and Service d'Etude et de Recherche sur les Lipoprotéines et l'Athérosclérose,** Institut Pasteur de Lille, 1, Rue du Prof. Calmette, B.P. 245, 59019 Lille, Cédex, France

Abstract In the present study, the relative positions of 11 anti-apolipoprotein B monoclonal antibodies have been mapped onto the surface of human low density lipoproteins by electron microscopy. As the epitopes recognized by these antibodies have been previously located on the primary sequence of apoB, these data provide a map of the configuration of the protein on the surface of the LDL. The first 89% of apoB-100 may be modeled as a thick ribbon that wraps once around the LDL, completing the encirclement by about amino acid residue 4050. The thickness of the ribbon is sufficient to penetrate the monolayer, so that it makes contact with the core. There is a kink in the ribbon beginning almost halfway along its length at approximately apoB-48. The C-terminal 11% of apoB constitutes the "bow," an elongated structure of about 480 residues, beginning at 4050 and stretching back into one hemisphere and then crossing the ribbon into the other hemisphere between residues 3000 to 3500, thus bringing sequences in the C-terminal portion of apoB-100 near to the suggested binding site for the LDL receptor. The C-terminal sequences may act as a negative regulator of LDL receptor binding, in agreement with Parhofer et al., 1992. *J. Clin. Invest.* **89:** 1931–1937, who reported the enhanced clearance from plasma of apoB-89-containing lipoproteins. It is proposed that in VLDL the bow could function to inhibit binding to the receptor; during lipolysis to form LDL, it is suggested that these C-terminal inhibitory sequences forming the bow would move sufficiently to allow interaction with the LDL-receptor.—**Chatterton, J. E., M. L. Phillips, L. K. Curtiss, R. Milne, J-C. Fruchart, and V. N. Schumaker.** Immunoelectron microscopy of low density lipoproteins yields a ribbon and bow model for the conformation of apolipoprotein B on the lipoprotein surface. *J. Lipid Res.* 1995. **36:** 2027–2037.

Supplementary key words electron microscopy • lipoprotein • LDL • structure

Apolipoprotein B-100 (apoB-100) is a large, single-chain glycoprotein composed of 4536 residues (1, 2) that is required for secretion of the triglyceride-rich very low density lipoproteins (VLDL) from the liver. It is also the only apolipoprotein not transferred between lipoprotein particles during the metabolic conversion of VLDL into low density lipoproteins (LDL). LDL are spherical particles consisting of a core containing mostly cholesteryl esters together with some triglyceride, surrounded by a monolayer of phospholipid and unesterified cholesterol in which is embedded a single copy of apoB-100 (reviewed in ref. 3). In spite of its great size, apoB-100 has not been resolved on the surface of intact, negative-stained LDL by electron microscopy (4, 5).

We have previously studied the conformation of apoB on intact LDL by immunoelectron microscopy (6), using apoB-specific monoclonal antibodies that attached to LDL and were clearly resolved in negative-stained samples. These monoclonal antibodies were used to determine the relative locations of specific regions of apoB on the intact LDL particle. By measuring the angular separations between all possible pairwise combinations

---

Abbreviations: VLDL, very low density lipoprotein; LDL, low density lipoprotein.

[1]Current address: Department of Biology, Massachusetts Institute of Technology, Cambridge, MA 02139.

[2]To whom correspondence should be addressed.

of six monoclonal antibodies, a three-dimensional model for apoB on the LDL surface was constructed. The results were consistent with a previously proposed model (5) in which apoB-100 formed a belt surrounding the LDL sphere. Further support for a belt-like model was suggested by electron microscopy of LDL in vitreous ice (7–9).

Support for the belt model for apoB-100 has also emerged from a study of the sizes of the lipoproteins secreted by hepatocytes transfected with plasmids encoding C-terminally truncated apoBs. The circumference of the lipoprotein core was found to be directly proportional to the length of the truncated apoB. This observation was consistent with a model for lipoprotein biosynthesis in which apoB determined the core circumference by encircling a droplet of nonpolar triglyceride and cholesteryl ester within the membrane of the endoplasmic reticulum. According to the model, when translation was completed, the C-terminus of apoB completed the encirclement, pulling the phospholipid monolayer around the core, and the nascent particle pinched off the membrane into the lumen of the endoplasmic reticulum, forming a lipoprotein with apoB wrapped once about its circumference, in contact with the core (10).

In the present work, data are presented specifying the locations of six additional monoclonal antibodies. One of the monoclonals previously mapped, MB44, consistently gave very broad distributions of angles with other monoclonal antibodies, and a high background of unbound antibodies was visible in electron micrographs involving this monoclonal. Accordingly, even though its position was consistent with our current model, we have removed MB44, leaving a total of eleven antibodies on our current map. In our original three-dimensional map, flattening of the LDL sphere on the electron microscope grid may have distorted the configuration of apoB-100. Such distortion would affect the measurements of the angle separating the epitopes recognized by the monoclonal antibodies. We reasoned that distortion of the measured distances between the antibodies would be greatest in the gap between the two ends of the belt as the belt was not covalently "buckled." To minimize the effects of distortion on the current map, the three most N-terminal antibodies were used to establish a three-dimensional coordinate system on the spherical model. Successive antibodies were then placed on the map by triangulation relative to the three most immediately previous antibodies. Thus, the current map was constructed one antibody at a time proceeding from the N- to the C-terminus.

The increase in resolution afforded by having 11 uniformly spaced monoclonal antibodies provides additional detail concerning the configuration of apoB on the LDL, allowing us to propose a ribbon and bow model, in which the C-terminal 11% of apoB-100 forming the bow may function to regulate access to the LDL-receptor binding site.

MATERIALS AND METHODS

Lipoproteins

LDL were isolated as previously described (6). In brief, a 1.019–1.063 g/ml fraction of fresh human plasma was prepared by first floating all lipoproteins with a density less than 1.063 g/ml, then centrifuging these lipoproteins at a density of 1.019 g/ml and collecting the bottom 1.5 ml. This crude LDL preparation was then further purified using an isopycnic gradient and the 1.0320–1.0366 g/ml fraction isolated for the electron microscope studies. Protease inhibitors (Polybrene, benzamidine, ε-amino caproic acid, and soybean trypsin inhibitor at final concentrations of 24 μg/ml, 2

TABLE 1. Angles between pairs of monoclonal antibodies bound to LDL[a]

	MB24	MB11	2D8	B4	B3	4G3	MB47	MB43	Bsol16	Bsol7
MB19	43[b]	45[b]	95	–	–	–	–	–	–	–
MB24	–	45[b]	86	157	–	–	–	–	–	–
MB11	–	–	57	120	113	–	–	–	–	–
2D8	–	–	–	74	69	132	–	–	–	–
B4	–	–	–	–	65	60	109	–	64	–
B3	–	–	–	–	–	104	155	–	–	–
4G3	–	–	–	–	–	–	54	96	43	–
MB47	–	–	–	–	–	–	–	52	48	67
MB43	–	–	–	–	–	–	–	–	76	73
Bsol16	–	–	–	–	–	–	–	–	–	111

[a]The standard errors of the angles listed in Table 1 ranged from 0.7% to 5.8%; the average standard error was 2.2%.
[b]Data from ref. 7.

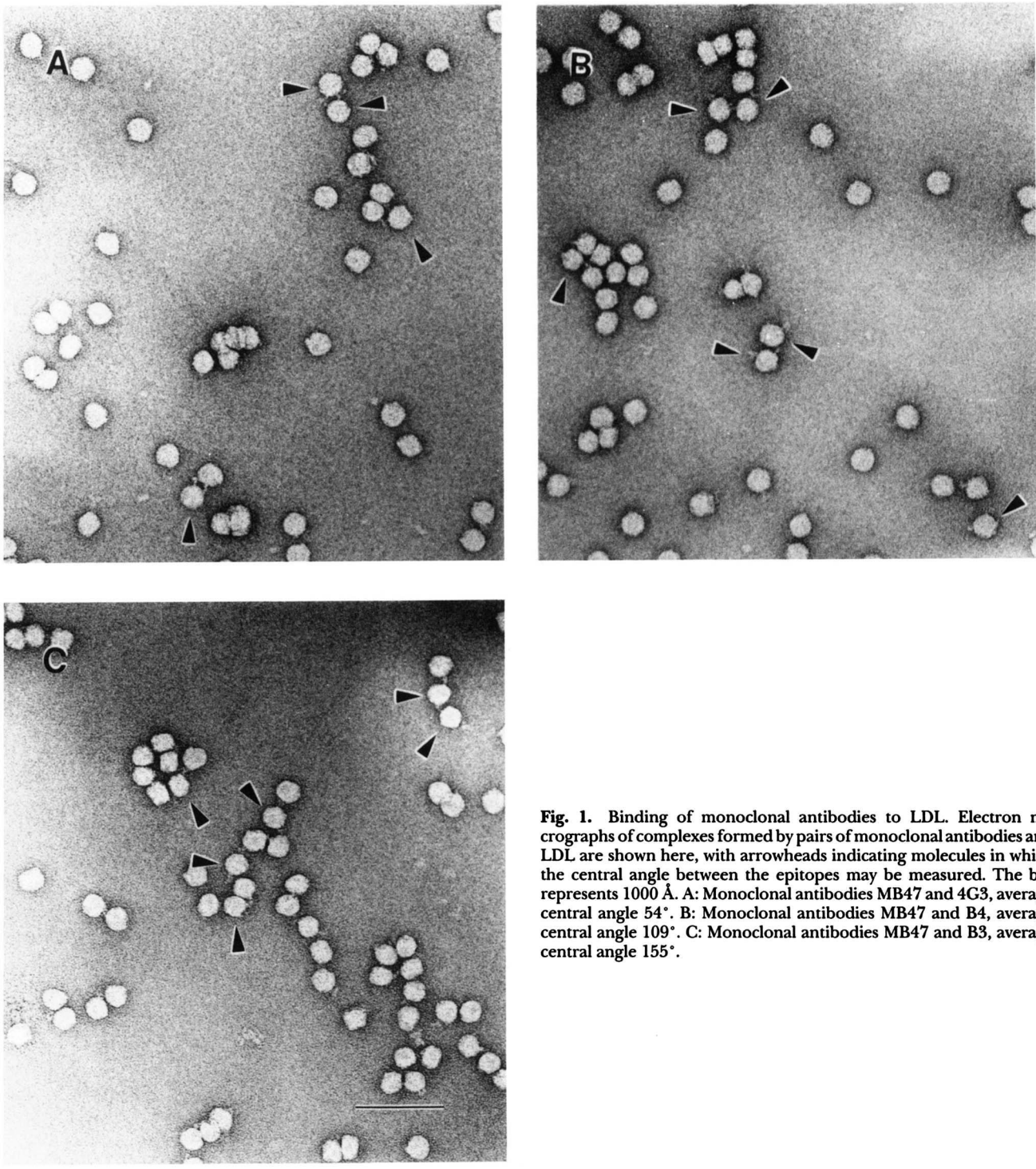

Fig. 1. Binding of monoclonal antibodies to LDL. Electron micrographs of complexes formed by pairs of monoclonal antibodies and LDL are shown here, with arrowheads indicating molecules in which the central angle between the epitopes may be measured. The bar represents 1000 Å. A: Monoclonal antibodies MB47 and 4G3, average central angle 54°. B: Monoclonal antibodies MB47 and B4, average central angle 109°. C: Monoclonal antibodies MB47 and B3, average central angle 155°.

mM, 5 mM, and 20 μg/ml, respectively) were added immediately after the blood was drawn. Nitrogen-saturated solutions and EDTA (0.04%) were used throughout the isolation to avoid oxidation. Anti-bacterial agents, 0.05% sodium azide and 0.005% gentamicin sulfate, were also present throughout the isolation. Lipoproteins were dialyzed into nitrogen-saturated 0.195 M NaCl, 0.04% EDTA, 0.05% sodium azide, 0.005% gentamicin sulfate, and stored under nitrogen at 4°C.

Electron microscopy

Samples were prepared and mounted essentially as previously described (6). For monoclonal antibody anti-Bsol7, which was reported to bind poorly to freshly prepared LDL (11), samples were incubated at higher

concentrations, 250–500 nM, than the 50–100 nM previously used. All samples were diluted to a final apoB concentration of 2.5 nM immediately before use. Electron microscopy was performed on a JEOL JEM 1200 EX electron microscope at 80 kV or a Hitachi H-7000 electron microscope at 75 kV at magnifications between 30,000 and 40,000 (calibrated using a diffraction grating replica). A Sigma-Scan digitizing board (Jandel Scientific, Corte Madera, CA) was used to record the coordinates of the three points along the LDL perimeter used for determining the central angle between the antibody binding sites, otherwise the analysis of the electron micrographs was performed as previously described (6).

Other techniques

Protein concentration was determined by the Markwell modification of the Lowry technique (12). The absence of apoB proteolysis was checked by sodium dodecyl sulfate-polyacrylamide gel electrophoresis using 5% acrylamide, 0.1% bisacrylamide gels, and the buffer system of Laemmli (13).

Computer program for mapping

The strategy for locating the relative positions of the monoclonal antibodies has been graphically illustrated (See Fig. 10 of ref. 3).

A computer program was written in Basic to calculate the coordinates of each monoclonal from the angles listed in **Table 1.** A spherical coordinate system was used and the monoclonal antibody closest to the N-terminus of apoB, MB19, was arbitrarily placed at the north pole, or $\theta = 0^\circ$ in polar coordinates. Proceeding from the N-terminus, the next monoclonal, MB24, was placed at 43°, 0°, where the latitude,[3] $\theta = 43^\circ$, was the measured angle between monoclonals MB19 and MB24 (Table 1), and the longitude, $\phi = 0$, was arbitrarily assigned. Thus, MB24 served a purpose analogous to Greenwich, England on Earth, as defining the prime meridian or 0° longitude. The position of the next monoclonal antibody, MB11, was located by triangulation from the angular separations from the other two, using the cosine rule of spherical trigonometry:

$$\cos^2(a) = \cos^2(b) + \cos^2(c) - 2\cos(b)\cos(c)\cos(A)$$

where a, b, and c were the measured angular separations between three epitopes forming the sides of a triangle on the surface of a sphere, and A was the dihedral angle formed at the vertex of the triangle between sides b and c. Thus, if the three angular distances a, b, and c, separating the three monoclonal antibodies were measured, the three dihedral angles, A, B, and C, of the spherical triangle were determined through permutations of the expression given above. From this information, the coordinates θ and ϕ were calculated. Thus, θ was always equal to the latitude or angular separation between any monoclonal antibody and MB19 located at the north pole; and ϕ was always equal to the longitude, conveniently calculated as the dihedral angle at the north pole between any monoclonal and MB24. The first time this calculation was used, however, there was an ambiguity, for two solutions are possible (that is, the third monoclonal, MB11, may be placed in either the western or eastern hemispheres). This ambiguity was resolved by arbitrarily placing MB11 in the western hemisphere. After the first three monoclonal antibodies were placed, successive monoclonals could be located uniquely, for the distance from a third epitope was always available to resolve the ambiguity. The final map produced by this method, however, may be a mirror image of the true map, a problem left to the future.

RESULTS

To measure the configuration of apoB on the LDL particle, the angles between pairs of anti-apoB monoclonal antibodies bound to the surface of the LDL were determined with the electron microscope. LDL were circular in projection, and antibodies were observed only when bound near the edge of the LDL where they displaced sufficient stain to be visualized through the negative contrast. As only antibodies lying in the plane of the grid are visualized by the negative stain technique, errors due to parallax are believed to be small. Complexes were selected in which two antibodies could be seen clearly contacting the same LDL near its periphery, and in which the LDL were circular with an apparent mean diameter of less than 300 Å. By selecting images in which the tips of the antibody contacted the LDL near its periphery, errors due to random superpositions were decreased. Selecting round, < 300 Å diameter LDL minimized errors due to distortion (flattening) of the LDL on the grid.

The angle measured at the center of the LDL separating the two antibody contact sites was characteristic for each pair of monoclonal antibodies. For example, complexes between LDL, monoclonal antibody MB47, and monoclonal antibodies 4G3, B4, or B3 were prepared and observed in the electron microscope (**Fig. 1**). In

[3]Using a conventional nomenclature frequently used for spherical coordinates, θ is the angular polar coordinate measured between the radial vector and the Cartesian z axis, and can be thought of as a measurement of latitude (on the Earth, the North Pole is at 90° N latitude, while in spherical polar coordinates the scale is shifted so that the North Pole is at 0° and the South Pole is at 180°). ϕ is the angle between the x axis and the projection of the radial vector on the x, y plane, and can be thought of as a measurement of the longitude (on Earth both east and west longitudes from 0° to 180° are used, while in spherical polar coordinates the scale runs eastward from 0° to 360°).

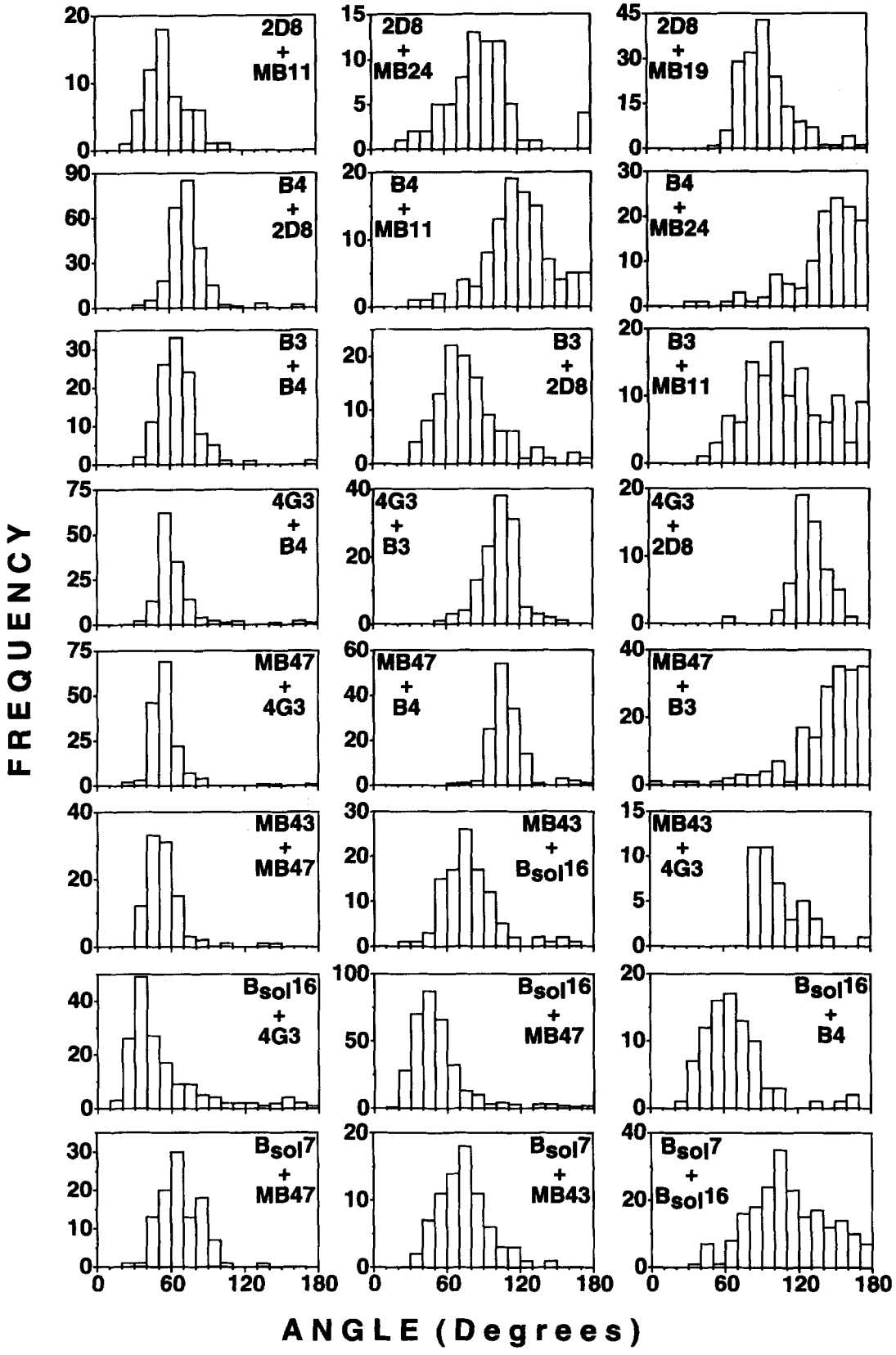

Fig. 2. Distributions of central angles measured between pairs of monoclonal antibodies bound to LDL. Each row contains data for the monoclonal antibody pairs used to determine the position of the common epitope. The first and second columns show the angles between the monoclonal antibody pairs that were used to determine the two possible positions for the common epitope; the third column shows the monoclonal antibody pairs used only for distinguishing between those two possible positions.

complexes formed between LDL, MB47, and 4G3, the two monoclonals bound relatively close together; their epitopes were separated by an average central angle of 54° (Fig. 1A). In contrast, in complexes between LDL, MB47, and B4, the average angular separation of the epitopes was 109° (Fig. 1B), twice that of the previous pair. In the case of complexes formed between LDL, MB47, and B3, the antibodies bound far apart, with an average angle of 155° (Fig. 1C) or three times that observed for the first pair. For MB47 and B3, angles of 180° were often seen. Histograms of the angles measured for these three antibody pairs are shown in **Fig. 2,** in the fifth row from the top. Both 4G3 and B4 gave well-defined peaks with MB47. The angle between B3 and MB47 was so large that both sides of the peak were not contained within the plot borders, as angles greater than 180° cannot be distinguished from the supplementary angles less than 180°.

To reduce the uncertainty introduced by measuring large angles, neighboring epitopes were selected in a stepwise fashion. The angles between MB19, MB24 and MB11, previously reported (6), were used to place the first three antibodies at the N-terminus of apoB, as described in Methods. After these had been placed, successive epitopes were located from the angles measured to their immediately preceding neighbors. The angles from the two closest epitopes determined two possible positions for the next epitope; the angle from a third was then used to distinguish between these two possibilities. Thus, MB47 was mapped by using the measured angles from 4G3, B4, and B3, whose positions had been previously established. The relatively well-defined angles from 4G3 and B4 determined two possible locations for MB47; one of these was about 90° from B3 while the other was about 150° from B3. The measured angle of 155° between MB47 and B3, though somewhat uncertain because of its size, readily distinguished between these two possibilities.

Histograms of previously unreported angles measured between various pairs of monoclonal antibodies used to construct the current map are provided in Fig. 2. Each row consists of the three pairs used to place a particular epitope; the first row positions 2D8, the second row B4, etc. The first two columns of Fig. 2 provide the distributions used to calculate the average angles between the antibody pairs used to solve for the two possible locations of the unknown epitope. The third column contains the distribution used only for distinguishing between these two possible locations. Table 1 summarizes the average angles measured for the pairs of monoclonal antibodies. In some cases outlier points were ignored in calculating these means; the average angle for the MB47/4G3 pair, for example, ignores angles greater than 100°.

Table 2 provides polar coordinates for the 11 monoclonal antibodies mapped to the surface of a sphere, calculated as described in Methods from the angular measurements listed in Table 1.

In addition to the monoclonal antibody pairs used in constructing the map, listed in Table 1, average angles (n > 50) were measured between a number of other monoclonal pairs; these included MB19/B4 (156°), MB19/4G3 (130°), MB19/MB47 (85° and 84°), MB19/MB43 (43°), MB19/Bsol16 (101°), MB24/MB47 (80°), MB24/Bsol16 (117°), MB11/MB47 (132°), MB11/Bsol16 (135°), B4/MB43 (146°), B3/MB43 (148°), and B3/Bsol16 (121°). Duplicate measurements of monoclonal antibody pairs in Table 1 not included because of greater error in these experiments were MB24/B4 (159°), MB11/B4 (116°), 2D8/B4 (77°), MB47/Bsol16 (48°), and MB43/Bsol16 (75°). Except for those angles measured "across the gap" between the N-terminus and the C-terminus (see Discussion), these additional angles were all consistent with the current map, within experimental error, demonstrating good internal consistency and strongly supporting the general features of the map.

DISCUSSION

Computer program to estimate cumulative error

The mapping technique used, which placed each epitope relative to its immediate neighbors, was designed to reduce error introduced by the flattening of LDL on the grid, which may result in the separation of the N- and C-terminal ends of apoB at the non-covalent N-ter-

TABLE 2. Polar coordinates of 11 monoclonal antibodies mapped to the surface of a sphere

Antibody	θ	f	Latitude[a]	Longitude[a]
MB19	0	0	90°N	0°
MB24	43	0	47°N	0°
MB11	45	293	45°N	67°W
2D8	102	289	12°	71°W
B4	141	210	51°S	150°W
B3	150	357	60°S	3°W
4G3	103	153	13°S	153°E
MB47	50	142	40°N	142°E
MB43	5	261	85°N	99°W
Bsol16	77	187	13°N	173°W
Bsol7	69	65	21°N	65°E

[a]Using a globe of the Earth and the small-sized "Post-it" Notes (Commercial Tape Division/3M, St. Paul), a model for the configuration of apoB on the surface of the LDL may be readily constructed from these data.

minal, C-terminal junction. This caution was clearly warranted as the extrapolated position by this mapping technique of the N-terminal epitopes relative to the C-terminal epitopes differed from measured angles between the epitopes; thus, the angle between MB47 and MB19 is 50° on the current map, but when directly measured was 85° (6). Because the current map was constructed in a stepwise fashion from the N-terminus, it might be argued that this difference arose from cumulative errors in the map. We do not believe this is the case for two reasons. First, all of the angles measured, including ones not used in constructing the map, gave results consistent with the map, except those measured "across the gap" between the N-terminus and the C-terminus. Second, to test the effect of cumulative errors, a computer program was written which automatically determined the positions of the epitopes but randomly varied the angles between ± 5% of their measured value. The angular distance from the mapped position was then determined. In 100 trials, the average cumulative error in the position of MB43 relative to its mapped position was 12.1°, suggesting that cumulative error is not responsible for the larger angles measured "across the gap" between the N-terminus and C-terminus. It seems more likely that when the LDL was distorted on the electron microscope grid, the two ends of apoB moved apart, resulting in an abnormally large measured angle between N- and C-terminal epitopes relative to their mapped positions. Cumulative errors would have little effect on the local features identified here, such as the more compact N-terminus, the "kink," and the "bow."

First 89% of apoB forms a ribbon encircling the LDL

The 11 epitopes recognized by the monoclonal antibodies used to construct the current model have been placed on the primary sequence of apoB, as shown in **Table 3,** usually within a stretch of about 100 amino acids. These 11 epitopes span essentially the entire length of apoB-100, from sequences near residue 71, close to the N-terminus, to sequences within residues 4521–4536 at the C-terminus, and are spaced at approximately 400–500 residue intervals, with the exception of the B3–4G3 interval, which is somewhat longer (747 residues) and the MB43–Bsol16 interval, which is considerably shorter (118 residues).

Figure 3 and **Figure 4** show the current map of the N-terminal 89% of apoB-100 on the LDL surface. For convenience, the epitope positions are expressed in the centile nomenclature, followed by the designation of the monoclonal antibody in parentheses. The N-terminus is exceptionally compact, with three epitopes, 2% (MB19), 11% (MB24), and 23% (MB11), spanning the initial 1000 residues of apoB, separated by only 45° (Fig. 3A). In contrast, the next 420 residues, from 23% (MB11) to 32% (2D8), extend apoB-100 by an additional 57° around the LDL (Fig. 3A); the next 407 residues, from 32% (2D8) to 41% (B4) extend apoB-100 another 74° around the LDL (Fig. 3B). Then, this progression around the sphere is interrupted by a "kink" between 41% (B4) and 50% (B3) in which the sequence moves back across the LDL surface in the general direction of the N-terminus (Fig. 3B). After this kink, apoB resumes its progression around the LDL, on a somewhat larger circle. As seen in Figs. 3B, 3C, and 3D, the epitopes at 50% (B3), 67% (4G3), 77% (MB47), and 89% (MB43) extend circumferentially around the LDL until the N-terminus is encountered. Thus, the first 89% of apoB-100 completely encircles the LDL, bringing the epitopes at 2% (MB19) and 89% (MB43) close together.

Figures 3E and 3F show two views along the horizontal rotation axis used in Figs. 3A–D; the epitopes can be seen to reside a little more in one "empty" hemisphere than the other; thus, apoB is not quite centered as it surrounds the sphere. The overall shape of the first 89% of apoB-100 is that of a kinked ribbon completely encircling the LDL.

Some projections of apoB form rectangular images

A recent cryo-electron microscopy investigation of LDL (9) found that the high density regions of LDL, probably representing apoB, could be described as a double disc, that is, rectangular images containing two high density bands (the double disk viewed from the side) that could be converted by a rotation of 90° into a circular image (the disk view from the top). Interestingly, some, though not all, of the circular projections (Fig. 4 panel A) of our connectivity map of the first 89% of apoB can be converted into a rectangular, double-banded structure by a rotation of approximately 90°, as shown in Fig. 4, panel B. Although we do not know the

TABLE 3. Primary sequence positions of the epitopes recognized by anti-apoB-100 monoclonal antibodies

Monoclonal Antibody	Epitope Location	Centile Position
MB19	71	2
MB24	405–539	10
MB11	995–1082	23
2D8	1438–1480	32
B4	1854–1878	41
B3	2239–2331	50
4G3	2980–3084	67
MB47	3429–3453, 3507–3523	77
MB43	4027–4081	89
Bsol16	4154–4189	92
Bsol7	4517–4536	100

Positions of epitopes were determined in references 11, 14, 15, and 16.

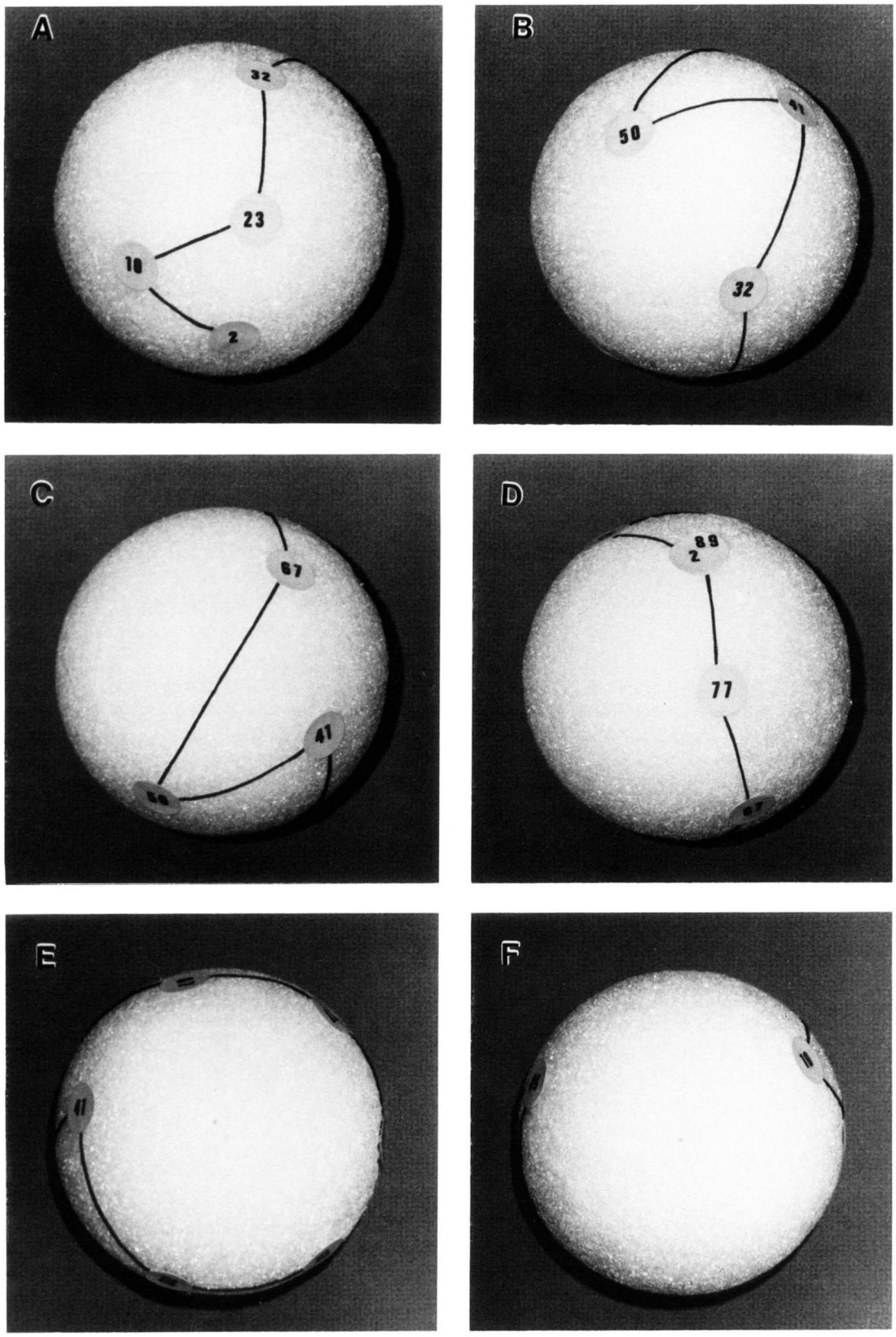

Fig. 3. Epitope mapping of the first 89% of apoB. Panels A, B, C, and D are related by sequential 90° rotations about a horizontal axis in the plane of the page. Panels E and F are views along this rotation axis. Each epitope is shown connected to the next epitope in the sequence of apoB by the arc from the great circle containing the two epitopes: a "connectivity map."

true path of apoB between the epitopes, the agreement is striking; it probably arises because the first 89% of apoB is a relatively uniform belt and thus the connectivity map of the epitopes represents a reasonable approximation of the mass distribution.

Average dimensions of the proposed ribbon model

A typical LDL has a radius of 100 Å, a molecular weight of 2.6 million, and is composed of 22% phospholipid and 11% cholesterol by weight (3). Taking the thickness of the surface monolayer to be 20 Å (3), the volume of the monolayer is 1.23 10^6 cm^3/mole. The phospholipid (0.984 ml/g) and cholesterol (1.021 ml/g) are sufficient to fill 70% of this volume, leaving 30% to be occupied by protein. The volume of apoB-100 (513,000 g/mol at 0.74 ml/g) would be just enough to occupy the remaining 30%. The volume occupied by apoB-89 is a little less. Thus, if apoB-89 were a thick, wedge-shaped ribbon, this ribbon would have to be 620 Å in length at the surface to encircle the LDL, and 60 Å in width at the surface to cover the remaining 30% of the surface area. The thickness of this wedge-shaped ribbon, 18 Å, can then be calculated from the requirement that it fills the volume occupied by apoB-89. Such a belt would surround the LDL, cover the surface not occupied by phospholipid monolayer, and make direct contact with the core.

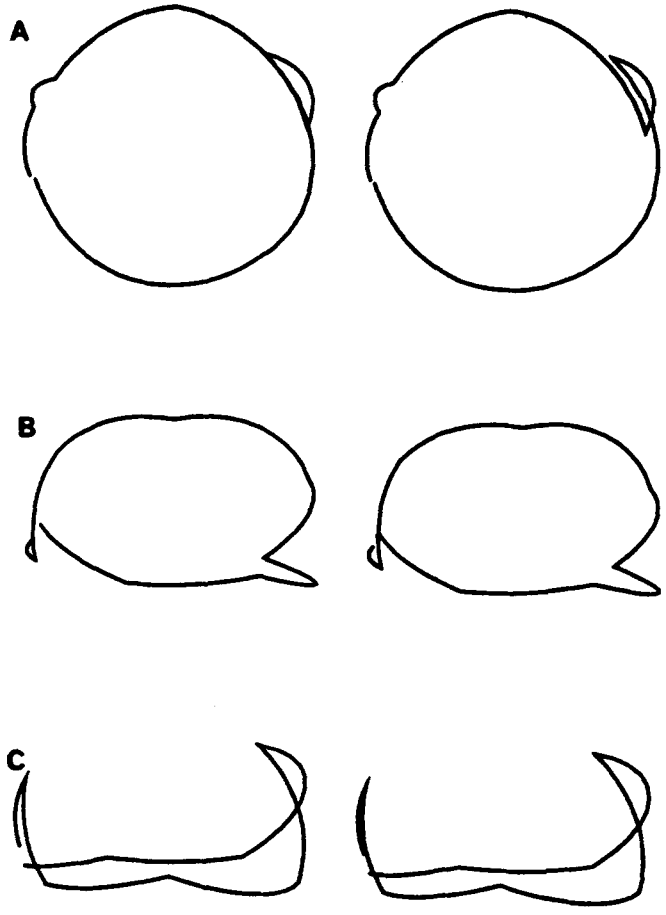

Fig. 4. Stereo views of the connectivity map of the first 89% of apoB. The lipid portion of the lipoprotein has been removed to describe the course of apoB. Panel A shows a circular projection. Panel B is rotated forward 90° relative to panel A to transform the circular projection into a rectangular double-banded projection. Panel C is rotated backward from panel A by about 45°.

Correspondence between the model and the primary sequence of apoB

Distinctive features on the current map correspond to regions of interest already identified on the basis of their characteristic primary structures. Thus, computer analysis of internal repeats in the sequence of apoB-100 have identified two clusters of 22 residue long amphipathic alpha helices between residues 2079 and 2428 and between 4150 and 4484 (17). A recent analysis of potential amphipathic structures in apoB-100 (18) also identified these two regions as having a high amphipathic helical potential, and suggested that these regions were involved in lipid binding. An N-terminal third region from amino acids 58–476, which contains amphipathic helices characteristic of globular proteins, was also identified, while the regions between these three helical domains were shown to be enriched in amphipathic beta structures (18). Therefore, the first, globular-protein-like helical domain would be consistent with the more compact configuration of the first 1000 residues on the map. The second amphipathic helical region of apoB-100 extending from about amino acid residues 2100 to 2600, encompasses the "kink" region, and the C-terminal third amphipathic helical region, from roughly 4150 to 4400, corresponds well to the elongated structure we refer to as the "bow." Most of the "ribbon" portion of apoB-100 consists of the intervening sequences rich in amphipathic beta structures.

Structure and possible function of the bow

The simple ribbon model is insufficient to describe the behavior of the final 11% of apoB. We refer to this C-terminal region as the "bow." As can be seen in **Fig. 5,** apoB-100 in the region from 89% (MB43) to 92% (Bsol16) stretches back in the general direction of its former path, away from the N-terminus, and extends into one hemisphere of the LDL. As these two epitopes are only separated by about 118 residues in the primary sequence but by 76° on the LDL surface, this portion of apoB-100 must be extremely elongated. If it were to be modeled as a cylinder arcing along the surface of the LDL, it would be about 140 Å long and 12 Å in diameter. From this epitope at 92% (Bsol16), the bow then crosses over the ribbon, with the C-terminal epitope (Bsol7) lying in the other hemisphere of the LDL (Fig. 5). The great circle connecting the epitopes at 92% (Bsol16) and

100% (Bsol7) crosses the ribbon near the epitope at 77% (MB47).

The structure of the bow may be related to a possible function. By moving back from the N-terminal, C-terminal junction and then crossing the ribbon, this elongated structure appears to bring elements in the C-terminus close to the epitope recognized by MB47, a monoclonal antibody that strongly inhibits binding of LDL to the LDL receptor (19, 20). Sequence homology to the apoE LDL receptor binding region also suggests that this region corresponds to the LDL receptor binding site on apoB-100 (21, 22). This evidence is suggestive only, as no intervening points have been placed on the path that apoB-100 follows from 92% (Bsol16) to 100% (Bsol7). However, it must cross the apoB-100 ribbon, and the shortest path between these epitopes intersects the LDL receptor binding region. Moreover, because LDL containing a truncated form of apoB that lacks the "bow" bind the LDL receptor more tightly than normal LDL (23, 24), it seems likely that the C-terminal sequences do interact with the LDL receptor binding region.

The kinetics of lipoprotein clearance in individuals with a truncated apoB-89 has been analyzed by Parhofer et al. (25). These authors found that the clearance of not just apoB-89-containing LDL and IDL were enhanced but also that of apoB-89-containing VLDL. This suggests a possible function for the bow. The bow may function as a negative regulator of LDL receptor binding, inhibiting binding to the LDL receptor in normal VLDL.

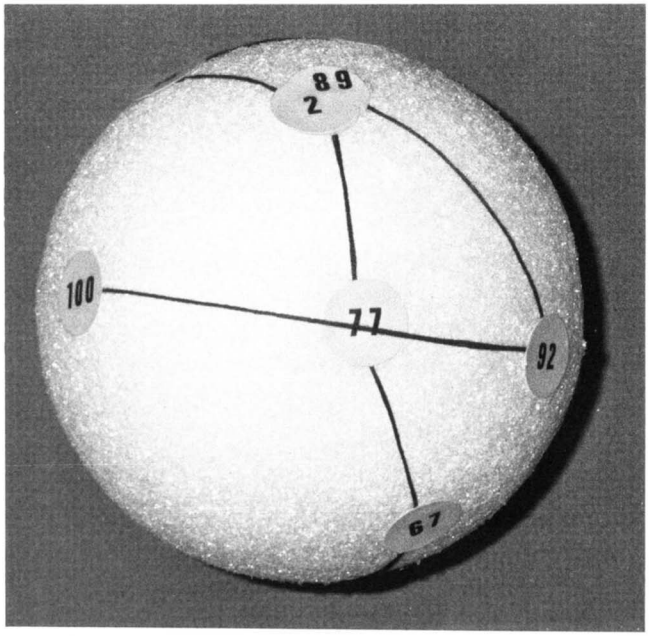

Fig. 5. The "bow" of apoB. The orientation is that of Fig. 3D. The C-terminal 11% of apoB-100 moves "backward" from the epitope at MB43 (89%), first into one hemisphere, Bsol16 (92%), and then crosses the ribbon near the LDL-receptor binding site and terminates in the other hemisphere at Bsol7 (100%).

Upon lipolysis to form VLDL remnants, IDL, and LDL, a conformational change in the bow, possibly mediated by the ends of apoB coming together, could lead to the unmasking of the LDL receptor binding site. If this hypothesis were correct, it would be predicted that, unlike normal large VLDL which do not bind the LDL receptor via apoB, large apoB-89-containing VLDL would display apoB-mediated clearance. This would explain the enhanced clearance of apoB-89-containing VLDL observed by Parhofer et al. (25) as being caused by a functional deletion. Furthermore, it may be suggested that mutations in the bow, particularly in the region between 4150 and 4400, might lead to abnormal binding to the LDL receptor by perturbing the normal regulatory function of the bow.

We would like to thank Duilio Cascio for his assistance in preparing the stereo diagrams of the apoB connectivity map and Christine Tsai for technical assistance. This work was supported by research grants NIH GM13914 (VNS) and Atherosclerosis Score Grant HL14197 (LKC). JEC was supported by USPHS grants HL07386 and CA09056.

Manuscript received 27 March 1995 and in revised form 24 May 1995.

REFERENCES

1. Knott, T. J., R. J. Pease, L. M. Powell, S. C. Wallis, S. C. Rall, Jr., T. L. Innerarity, B. Blackhart, W. H. Taylor, Y. Marcel, R. Milne, B. Wilson, and J. Scott. 1986. Complete protein sequence and identification of structural domains of human apolipoprotein B. *Nature.* **323:** 734–738.
2. Yang, C-Y., S-H. Chen, S. H. Gianturco, W. A. Bradley, J. T. Sparrow, M. Tanimura, W-H. Li, D. A. Sparrow, H. De Loof, M. Rosseneu, F-S. Lee, Z-W. Gu, A. M. Gotto, Jr., and L. Chan. 1986. Sequence, structure, receptor-binding domains and internal repeats of human apolipoprotein B-100. *Nature.* **323:** 738–742.
3. Schumaker, V. N., M. L. Phillips, and J. E. Chatterton. 1994. Apolipoprotein B and low-density lipoprotein structure: implications for biosynthesis of triglyceride-rich lipoproteins. *Adv. Protein Chem.* **45:** 205–248.
4. Shen, M. S., R. M. Krauss, F. T. Lindgren, and T. M. Forte. 1981. Heterogeneity of serum low density lipoproteins in normal human subjects. *J. Lipid Res.* **22:** 236–244.
5. Phillips, M. L., and V. N. Schumaker. 1989. Conformation of apolipoprotein B after lipid extraction of low density lipoproteins attached to an electron microscope grid. *J. Lipid Res.* **30:** 415–422.
6. Chatterton, J. E., M. L. Phillips, L. K. Curtiss, R. W. Milne, Y. L. Marcel, and V. N. Schumaker. 1991. Mapping apolipoprotein B on the low density lipoprotein surface by immunoelectron microscopy. *J. Biol. Chem.* **266:** 5955–5962.
7. Atkinson, D. 1989. Electron microscopy of unstained frozen hydrated low density lipoprotein (LDL). *Biophys. J.* **55:** A208 (Abstract).
8. Spin, J. M., and D. Atkinson. 1993. Structure of low density lipoprotein in vitreous ice. *Biophys. J.* **64:** A286 (Abstract).
9. Van Antwerpen, R., and J. C. Gilkey. 1994. Cryo-electron

microscopy reveals human low density lipoprotein substructure. *J. Lipid Res.* **35:** 2223–2231.
10. Spring, D. J., L. W. Chen-Liu, J. E. Chatterton, J. Elovson, and V. N. Schumaker. 1992. Lipoprotein assembly: apolipoprotein B size determines lipoprotein core circumference. *J. Biol. Chem.* **267:** 14839–14845.
11. Chen, P-F., Y. L. Marcel, C-Y. Yang, A. M. Gotto, R. W. Milne, J. T. Sparrow, and L. Chan. 1988. Primary sequence mapping of human apolipoprotein B-100 epitopes: comparisons of trypsin accessibility and immunoreactivity and implication for apoB conformation. *Eur. J. Biochem.* **75:** 111–118.
12. Markwell, M. A. K., S. M. Haas, L. L. Bieber, and N. E. Tolbert. 1978. A modification of the Lowry procedure to simplify protein determination in membrane and lipoprotein samples. *Anal. Biochem.* **87:** 206–210.
13. Laemmli, U. K. 1970. Cleavage of structural proteins during the assembly of the head of bacteriophage T4. *Nature.* **227:** 680–685.
14. Young, S. G., and P. A. Hubl. 1989. An ApaLI restriction site polymorphism is associated with the MB19 polymorphism in apolipoprotein B. *J. Lipid Res.* **30:** 443–449.
15. Pease, R. J., R. W. Milne, W. K. Jessup, A. Law, P. Provost, J-C. Fruchart, R. T. Dean, Y. L. Marcel, and J. Scott. 1990. Use of bacterial expression cloning to localize the epitopes for a series of monoclonal antibodies against apolipoprotein B-100. *J. Biol. Chem.* **265:** 553–568.
16. Young, S. G., R. K. Koduri, R. K. Austin, D. J. Bonnet, R. S. Smith, and L. K. Curtiss. 1994. Definition of a nonlinear conformational epitope for the apolipoprotein B-100-specific monoclonal antibody, MB47. *J. Lipid Res.* **35:** 399–407.
17. De Loof, H., M. Rosseneu, C-Y. Yang, W-H. Li, A. M. Gotto, Jr., and L. Chan. 1987. Human apolipoprotein B: analysis of internal repeats and homology with other apolipoproteins. *J. Lipid Res.* **28:** 1455–1465.
18. Segrest, J. P., M. K. Jones, V. K. Mishra, G. M. Anantharamaiah, and D. W. Garber. 1994. ApoB-100 has a pentapartite structure composed of three amphithatic α-helical domains alternating with two amphipathic β-strand domains: detection by the computer program LOCATE. *Arterioscler. Thromb.* **14:** 1674–1685.
19. Young, S. G., J. L. Witztum, D. C. Casal, L. K. Curtiss, and S. Bernstein. 1986. Conservation of the low density lipoprotein receptor-binding domain of apoprotein B. Demonstration by a new monoclonal antibody, MB47. *Arteriosclerosis.* **6:** 178–188.
20. Milne, R., R. Theolis, R. Maurice, R. J. Pease, P. K. Weech, E. Rassart, J-C. Fruchart, J. Scott, and Y. Marcel. 1989. The use of monoclonal antibodies to localize the low density lipoprotein receptor-binding domain of apolipoprotein B. *J. Biol. Chem.* **264:** 19754–19760.
21. Knott, T. J., S. C. Rall, T. L. Innerarity, S. F. Jacobson, M. S. Urdea, B. Levy-Wilson, L. M. Powell, R. J. Pease, R. Eddy, H. Nakai, M. Byers, L. M. Priestly, E. Robertson, L. B. Rall, C. Betscholtz, T. B. Shows, R. W. Mahley, and J. Scott. 1985. Human apolipoprotein B: structure of carboxyl-terminal domains, sites of gene expression, and chromosomal location. *Science.* **230:** 37–43.
22. Law, A., and J. Scott. 1990. A cross-species comparison of the apolipoprotein B domain that binds to the LDL receptor. *J. Lipid Res.* **31:** 1109–1120.
23. Krul, E. S., M. Kinoshita, P. Talmud, S. E. Humphries, S. Turner, A. C. Goldberg, K. Cook, E. Boerwinkle, and G. Schonfeld. 1989. Two distinct truncated apolipoprotein B species in a kindred with hypobetalipoproteinemia. *Arteriosclerosis.* **9:** 856–868.
24. Linton, M. F., R. W. Farese, and S. G. Young. 1993. Familial hypobetalipoproteinemia. *J. Lipid Res.* **34:** 521–541.
25. Parhofer, K. G., H. R. Barrett, D. M. Bier, and G. Schonfeld. 1992. Lipoproteins containing the truncated apolipoprotein, apoB-89, are cleared from human plasma more rapidly than apoB-100-containing lipoproteins in vivo. *J. Clin. Invest.* **89:** 1931–1937.